Article

Not peer-reviewed version

Fabrication and Characterization of Tissue-Engineered Carboxymethyl Cellulose Scaffolds Containing Spider Silk-Derived Fibroin Protein for Osteogenic Differentiation

Woong Jin Lee , Kyoungjoo Cho , Aaron Youngjae Kim , Gyung Whan Kim *

Posted Date: 26 June 2023

doi: 10.20944/preprints202306.1795.v1

Keywords: fibroin, scaffold; carboxymethyl cellulose (CMC); osteocyte; regenerative medicine

Article

Fabrication and Characterization of Tissue-Engineered Carboxymethyl Cellulose Scaffolds Containing Spider Silk-Derived Fibroin Protein for Osteogenic Differentiation

Woong Jin Lee [1,#], Kyoungjoo Cho [2,#], Aaron Youngjae Kim [1,3] and Gyung Whan Kim [1,*]

[1] Department of Neurology, College of Medicine, Yonsei University, Seoul, South Korea; osang0616@yuhs.ac
[2] Department of Life Science, Kyonggi University, Suwon, South Korea; kcho0611@kgu.ac.kr
[3] Weill Cornell Medicine-Qatar, Doha, Qatar; Yok2019@qatar-med.cornell.edu
* Correspondence: gyungkim@yuhs.ac
# The authors equally contributed to this article.

Abstract: This study aimed to investigate the characteristics of composite scaffolds in combination of fibroin and carboxymethyl cellulose (CMC) in bone tissue engineering. Fibroin is a useful biomaterial and is a major component of silk yarns composed of fibrous proteins. Improving for binding efficiency in bone formation after implanted scaffold, CMC was added to fibroin. CMC could improve injectable characters in bone substitutes by adding in scaffold material, fibroin. The porous shapes, porosity, surface wettability, water absorption, and thermal properties of the CMC added fibroin scaffold were better than fibroin only scaffold. For tissue engineering of bone marrow mesenchymal stem cells (BMSCs), BMSCs isolated from mice were seeded onto the scaffold, and the cell proliferation rate was measured. alkaline phosphatase activity in BMSCs was higher in the scaffold containing CMC than that in the scaffold containing fibroin alone. The expression levels of osteocyte marker genes and proteins were increased in the CMC scaffold. The biocompatibility and hydrophilicity of CMC scaffolds play important roles in the growth and proliferation of osteocytes. Furthermore, the CMC scaffold design proposed in this study could play an important role in facilitating cartilage, ossification, and nerve differentiation of BMSCs.

Keywords: fibroin; scaffold; carboxymethyl cellulose (CMC); osteocyte; regenerative medicine

1. Introduction

The scaffold plays an important role in the growth of cells seeded in a porous structure and in mediating cell migration from the periphery of the tissue. Most cells in the human body are adherent cells, and if there is no place to attach, the cells cannot grow and die. Owing to these characteristics, many difficulties are encountered during cell therapy, and scaffolds have been introduced and widely used to solve this problem. A scaffold is used as a carrier for cells. It delivers high concentrations of cells to specific tissues and organs of the human body with high efficiency [1]. An ideal scaffold for tissue engineering applications should sustain cell function and proliferation, sufficiently aid in cell adhesion, and have a porous structure that can aid in the diffusion of oxygen and nutrients from cells. In addition, it should be able to interact with the active groups on the surface of biochemical reagents and biomaterials, receptors on the cell surface, and growth factors. It must maintain its shape and be structurally stable against in vivo chemical changes. In general, scaffolds with three-dimensional pores are composed of natural and synthetic polymers, ceramics, metals, and composite materials. Among these, many types of naturally derived scaffolds are used for bioengineering purposes, and scaffolds made of biomaterials play an important role in cellular survival in tissue engineering. Naturally derived polymers include alginate, protein, collagen (gelatin), keratin, fibrin, albumin, gluten, elastin, hyaluronic acid, cellulose, starch, chitin, scleroglucan, elcinan, pectin (tectinic acid), galactan, curdlan, gellan, levan, dextran, pullulan, heparin, silk, chondroitin sulfate, and polyalkanoates [2–4]. Naturally derived polymers have garnered significant interest because of their

Preprints (www.preprints.org) | NOT PEER-REVIEWED | Posted: 26 June 2023 doi:10.20944/preprints202306.1795.v1

relatively good biocompatibility, abundance, commercial availability, easy processing, and easy approval by the Food and Drug Administration (FDA). Fibroin, a naturally derived polymer, is a hydrothermally insoluble protein that composes silk yarn. It is characterized as a hard protein [5]. In particular, it comprises seventeen types of amino acids, including tyrosine and serine, along with a large amount of glycine and alanine, and is stable against proteolytic enzymes. It contains 72 - 81 % of cocoon fibers [6,7]. The liquid silk of the silkworm is discharged from the vomit tube to outside the body, where the globular fibroin transforms into a β-type fibrous molecule and simultaneously loses its water solubility. Spider silk belongs to the fibroin protein family [8–10]. Carboxy-methyl cellulose (CMC) is one of substitute materials playing a binding role in bone formation of implanted scaffold [11]. CMC has been applied to improve injectable characters in various scaffold materials including bone substitutes [12].

In this study, CMC was added to fibroin to obtain a scaffold, and the physical properties of the CMC polymer were mechanically, chemically, and biologically analyzed. This study focused on the facilitating effect of the CMC added scaffold on bone differentiation. Our results showed that the CMC scaffold could play an important role in facilitating cartilage, ossification, and nerve differentiation of BMSCs, which indicates a potential application of such scaffolds in regenerative medicine.

2. Materials and Methods

2.1. Fabrication of CMC Porous Scaffold Containing Silk Fibroin

A schematic of silk fibroin/CMC/gelatin scaffold production is shown in Figure 1. We attempted to determine conditions that could provide an optimal environment for cell growth by adding CMC, gelatin, and crosslinking agents to silk fibroin and varying the concentration of each component. To remove sericin from the silk protein obtained from the spider silk, it was stirred with 0.02 M sodium carbonate solution at 100 °C for 20 min [13,14]. Thereafter, sericin was eliminated by repeated washing with tertiary distilled water. After drying the mixture in an oven, a silk fibroin solution was prepared by dissolving 10 g of silk fibroin in 9.3 M LiBr solution at 70 °C for 2 h 30 min and dialyzed on a cellulose membrane [15–17]. Tertiary distilled water was replaced every 6 h for three days to eliminate LiBr. The supernatant was obtained after centrifugation at 9000 rpm for 20 min at 4 °C. Protein concentration was measured using the Bradford standard assay [18]. A total of 50 % of the silk fibroin solution purified via the aforementioned method was placed into a 24-well plate, and 0%, 10%, 20%, and 50% of the CMC solution was dispensed, respectively. Then, to induce the formation of a porous sponge, a scaffold was prepared in which 4 % gelatin solution and 2.5 % glutaraldehyde mixed aqueous solution (used as a crosslinking agent) were added to the aforementioned solution. The scaffold was stored at 4 °C and -20 °C for 8 h and cooled at -80 °C for 24 h. Subsequently, cross-linking in the scaffold was inhibited using 100 % glycine, followed by washing five times with tertiary distilled water to remove glycine solution. After drying in a vacuum oven at 25 °C for at least one week to remove the residual solvent, ethylene oxide (EO) sterilization was performed. The scaffolds were used for cell culture experiments after sterilization [19–21].

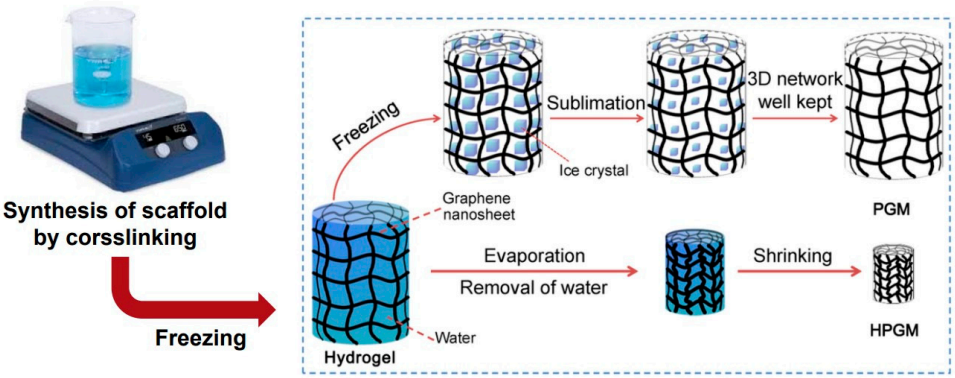

Figure 1. Fabrication of CMC porous scaffolds containing silk fibroin. Schematic diagram of the fabrication process of fibroin/CMC hybrid scaffolds obtained by freeze-drying method.

 doi:10.20944/preprints202306.1795.v1

2.2. Surface Observation and Porosity Analysis of Scaffolds

The surface and inner porous morphologies of the porous support prepared via the aforementioned method were observed using a scanning electron microscope (SEM, JSM-6400, JEOL, Japan). The shape of the pores was confirmed using a photograph captured by cutting the scaffold with a scalpel to a size of 5 mm × 5 mm × 1 mm and coating using plasma sputtering. The pore size and distribution, average pore diameter, and porosity of the prepared porous support were measured using a mercury porosimeter [22].

2.3. X-ray Photoelectron Spectroscopy (XPS) Analysis

X-ray photoelectron spectroscopy (XPS) is used for analyzing photoelectrons generated by irradiating X-rays on the surface of a sample. When X-rays are projected onto the surface of a sample, electrons in the atoms receive energy and are ejected. If the kinetic energy of an electron is measured, and the unique work function of each element is known, the binding energy can be measured. Using the binding energy measured in this manner, it is possible to determine the type of material present on the surface of the sample. Such surface analysis can identify elements, chemical bonding states, and energy levels of surfaces and interfaces from the surface to a depth of approximately 20 Å for hard materials such as metals and 100 Å for organic or polymeric materials. For the XPS analysis, Thermo VG Scientific K-alpha (Waltham, MA, USA) was used [23].

2.4. Structural Analysis Using H-NMR

Nuclear magnetic resonance spectroscopy is used for measuring the spin of atoms constituting a sample. The structure of the scaffold was examined via nuclear magnetic resonance. In this study, the spin of hydrogen was investigated and confirmed using a spectrometer. Each sample (500 l) was prepared to obtain a concentration of 10 mg/ml, and D2O (Cambridge Isotope Laboratories, Inc.) was used as the solvent [24].

2.5. Differential Scanning Calorimetry Analysis

Differential scanning calorimetry was used to observe the thermal behavior of the scaffold with respect to the fibroin content. The change in thermal properties was measured by applying heat to the fibroin/CMC support. The temperature was increased from room temperature to 100 °C [25]. For analysis, the temperature increase rate was set to 10 °C, and measurements were made under conditions involving the nitrogen stream.

2.6. Hydrophilicity Measurement

To examine the hydrophilic effect of the porous support according to the fibroin content, trypan blue dye was dropped onto the support, and the degree of absorption over time was observed. The effect of dye penetration was analyzed 20, 40, 60, 80, and 100 min after dropping the trypan blue dye by measuring the contact angle [26].

2.7. Water Absorption Rate Measurement

To measure the water absorption capacity of the prepared scaffolds, the following experiment was performed. First, the initial weight of the scaffold was measured, and it was left at room temperature in 10 ml of water for 3, 5, 7, and 10 days. After eliminating moisture from the surface of the scaffold that had absorbed water, the weight was measured, and the water absorption rate was measured by substituting it in the water uptake [27]. All experiments were performed thrice under the same conditions.

2.8. Isolation and Culture of BMSCs

Primary BMSCs were isolated and cultured using a previously reported method [28]. After cutting the thigh of a Fischer rat (female, three-week-old), 2–3 ml of bone marrow was collected using an 18-gauge needle. The collected bone marrow was diluted twice with culture solution to 50 % Percoll (Sigma Aldrich, MJ, USA), and slowly dropped into the gradual gradient solution to prevent mixing with the Percoll layer. The solution was centrifuged at 280 g for 25 min to obtain separate layers of red blood cells, Percoll, other cells, and plasma. Using a micropipette, only the cell layer was

 doi:10.20944/preprints202306.1795.v1

separated, diluted again with culture medium, and centrifuged at 150 g for 10 min. Subsequently, the cells were washed twice or thrice with the culture medium, the supernatant was removed, and the separated cells were treated with 10% fetal bovine serum (FBS, Gibco, MA, USA) and antibiotics (100 unit/ml penicillin and 100 μg/ml streptomycin, Gibco). The cells were cultured in Dulbecco's modified Eagle's medium (DMEM; low glucose, Gibco, USA) in a culture flask to obtain a density of 2x104 cells/cm2. The cells were cultured once every three days and subcultured once every seven days [29]. The isolated BMSCs were verified through von Kossa staining at DIV 0, 6, 9, and 15.

2.9. MTT Assay

3-(4,5-dimethythiazol-2-yl)-2,5-diphenyl-tetrazolium bromide (MTT, Sigma-Aldrich, USA) was used to evaluate the cytotoxicity of the prepared scaffolds. BMSCs were used for cytotoxicity evaluation. The cells were injected into a 96-well plate with the prepared scaffold to obtain a density of 1.3 × 105 cells/ml, followed by culturing in an incubator for 24 h. After 24 h, the treated supernatant was removed, and 200 μg/ml of the MTT solution was added, followed by incubation for 1 h and 30 min at 37 °C in the dark (the light was blocked). Subsequently, the MTT solution was removed, and the cells were washed twice with PBS. After washing, 200 μl of DMSO (Sigma-Aldrich, USA) was injected. The reaction was performed for 30 min. Cytotoxicity was evaluated by measuring the absorbance at a wavelength of 570 nm using a microplate reader (Thermo Fisher Scientific, MA, USA) [30].

2.10. Alkaline Phosphatase Assay

After inoculation of BMSCs on fibroin/CMC scaffolds, the activity of alkaline phosphatase assay (ALP) specifically expressed in osteoblasts was measured using the TRACP & ALP kit (Takara Bio Inc., Japan) to confirm differentiation into osteocytes according to CMC content. After removing the culture solution on days 1, 3, 7, and 14 and washing the cultured sample with physiological saline, 500 μl of the extract solution was mixed and stirred for 1 h. After centrifuging the mixture at 13000 rpm for 10 min, the supernatant was collected, mixed with the substrate solution and the mixture in a 1:1 ratio, and incubated at 37 °C for 1 h. Then, 0.9 N NaOH was added to stop the enzymatic reaction, and the absorbance was measured at 405 nm by adding 100 μL of each reaction solution [31].

2.11. Immunofluorescence Staining

Immunofluorescence staining was performed on cultured mesenchymal stem cells. To increase cell permeability, 0.2% Triton X-100 was added and reacted at room temperature for 15 minutes. Normal goat serum was then used to suppress non-specific reactions at 37°C for 1 hour, and primary antibodies were diluted in an appropriate ratio and incubated at 37°C for 1 hour. After incubation, the secondary antibody was added following three 5-minute washes with PBS. The secondary antibody was prepared by diluting FITC (Fluorecein isothiocynate)-conjugated goat antimouse IgG (Zymed, San Francisco, USA, 1:50) and TRITC (tetramethyrhodamin isothiocynate)-conjugated IgG (Zymed, San Francisco, USA, 1:30), and reacted at 37°C for 1 hour. After three additional washes with PBS, Hoechst 33258 (Sigma, St. Louis, USA, 1 μg/ml) was used for counterstaining at room temperature for 15 minutes, followed by sealing with Fluorescence medium and observation under a fluorescence microscope.

2.12. Alizarin Red Staining

Calcium mineralization was determined by Alizarin Red S staining. BMSC cells were then incubated in the experimental media that osteogenic differentiation medium. During the incubation, the media was changed every 2 days. After that, the BMSC cells were fixed with 10% formaldehyde and stained with Alizarin Red S in deionized water (pH = 4.1~4.3) for 1h at 25 ℃. After removing the Alizarin Red S by aspiration, the BMSC cells were washed three times with deionized water. For quantification, Alizarin Red S dyed the cells were destained with cetylpyridinium chloride, then the absorbance value was monitored at 450 nm using a microplate reader.

2.13. Western Blotting Analysis

Preprints (www.preprints.org) | NOT PEER-REVIEWED | Posted: 26 June 2023 doi:10.20944/preprints202306.1795.v1

After extraction with RIPA buffer, the protein was quantitatively analyzed using the bicinchoninic acid (BCA) assay. Based on this, 100 μg of protein was used for electrophoresis. Each protein sample mixed with a pre-stained protein marker (Bio-Rad, CA, USA) and loading buffer was denatured at 95 °C for 5 min, electrophoresed on 12.5 % SDS-PAGE gel, and then transferred to a nitrocellulose membrane (Bio-Rad, USA). After blocking the nitrocellulose membrane in a membrane blocking solution (Zymed, CA, USA) for 1 h, each antibody was diluted in a 400:1 ratio in the blocking solution; the reaction was carried out for 90 min. The reaction with the secondary antibody (HRP-conjugated anti-mouse IgG, Santa Cruz Biotechnology, TX, USA) was performed for 1 h. Detection was performed using an ECL chemiluminescence detection kit (Amersham, NJ, USA) [32].

3. Results

3.1. Fabrication of CMC Porous Scaffold and Analysis of the Scaffold Surface

Porous support containing fibroin was prepared using the solvent-casting freeze drying method. The external shape was identical to that of the silicone mold, and no shrinkage, swelling, holes with irregular sizes or other defects were observed (Figure 1).

An SEM image of the prepared porous fibroin/CMC scaffold is shown in Figure 2. The porous shapes of the inner and side surfaces of the support appeared to be similar to those of the salt particles. No significant morphological difference was observed between the support containing fibroin and the porous morphology without fibroin (Figure 2).

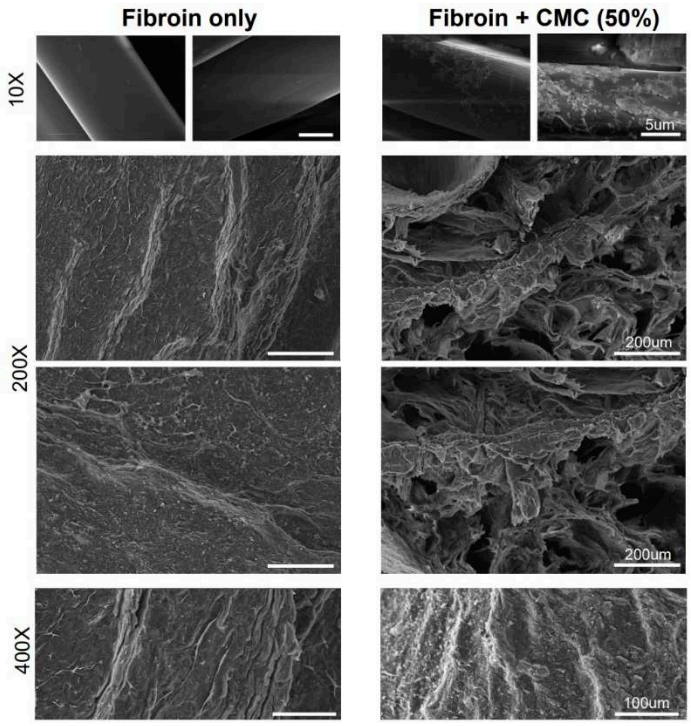

Figure 2. SEM micrographs of fibroin/CMC scaffolds developed via freeze-drying.

3.2. Mechanical Analysis of the Fibroin/CMC

To fully elucidate the functional groups and interactions on the CMC surface, we performed XPS measurements of fibroin and fibroin/CMC (Figure 3A).

Preprints (www.preprints.org) | NOT PEER-REVIEWED | Posted: 26 June 2023 doi:10.20944/preprints202306.1795.v1

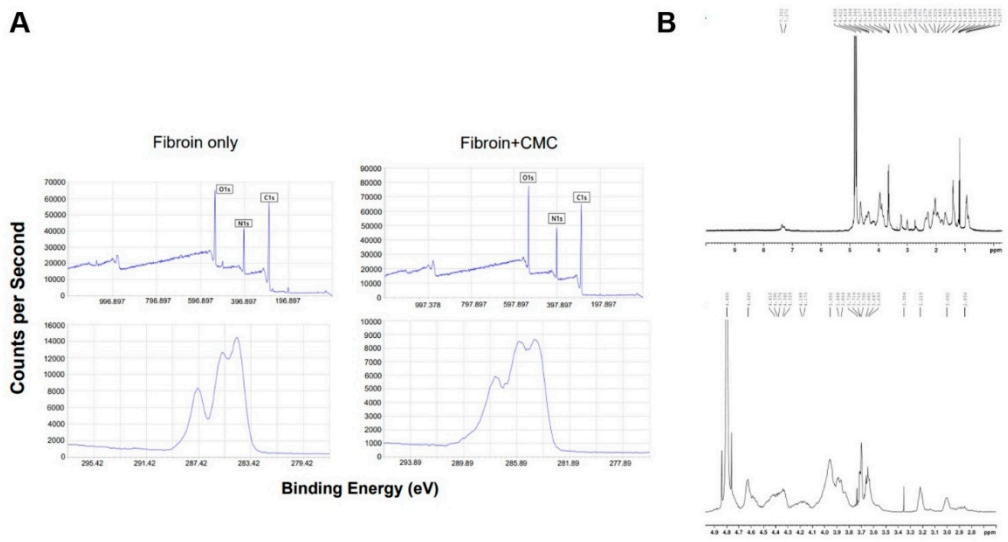

Figure 3. Mechanical analysis of the CMC. (A) The XPS survey spectra of the fibroin scaffold before and after the addition of CMC in X-ray photoelectron spectroscopy (XPS). (B) H NMR spectra were measured in fibroin (upper) and fibroin/CMC scaffold (lower).

The broad-scan spectrum showed three sharp peaks corresponding to fibroin (C 1s, O 1s, and N 1s) consisting to the previous reports [33]. This XPS spectrum was consistent with the chemical structure of polysaccharide CMC; three peaks (C1s, N1s, and O1s) corresponding to fibroin/CMC were observed. The presence of C1s, O1s, and N1s peaks at each eV demonstrated the successful integration of CMC into fibroin. The XPS spectra corresponding to the fibroin/CMC membrane surface in the C1s, O1s, and N1s regions showed the presence of an organic polysaccharide shell. As expected, the spectrum primarily demonstrated signals corresponding to carbon (C1s) and oxygen (O1s).

The structure of each compound was confirmed using the H-NMR spectrum, and the degree of substitution of the catechol group was evaluated by comparing the peak areas corresponding to the proton of the catechol group (3H, 6.75-6.88 ppm) and the proton of the acetyl group (3H, 2.1-2.25 ppm) (Figure 3B) A typical characteristic peak was detected in the fibroin NMR spectrum (Figure 3B, upper). On the other hand, the H-NMR spectrum of fibroin/CMC presented that a catechol group was introduced into fibroin (Figure 3B, lower) In the synthesized fibroin/CMC, a peak of the catechol group was observed near 7 ppm, and fibroin/CMC was well synthesized, as demonstrated by this new peak corresponding to the catechol group. The change in the substitution degree of the catechol group in fibroin/CMC was observed according to the amount of CMC in an aqueous solution of pH 5.5. As the amount of CMC increased during the reaction, the degree of substitution increased. However, no significant change was observed at an input amount of 1 g or more. In addition, the substitution degree of catechol group was changed when increasing the pH from 5.5 to 7.5 by fixing the input amount of CMC to 1 g. The amount of CMC (1 g) and pH (6.5) were fixed as the reaction conditions for fibroin/CMC with a maximum degree of substitution of 38.6 % (Figure 3B).

3.3. Properties of the Fibroin/CMC

The mercury porosimetry analysis showed that there is a minor difference in porosity distribution when the content of fibroin was approximately 50% (Figure 4A).

Preprints (www.preprints.org) | NOT PEER-REVIEWED | Posted: 26 June 2023 doi:10.20944/preprints202306.1795.v1

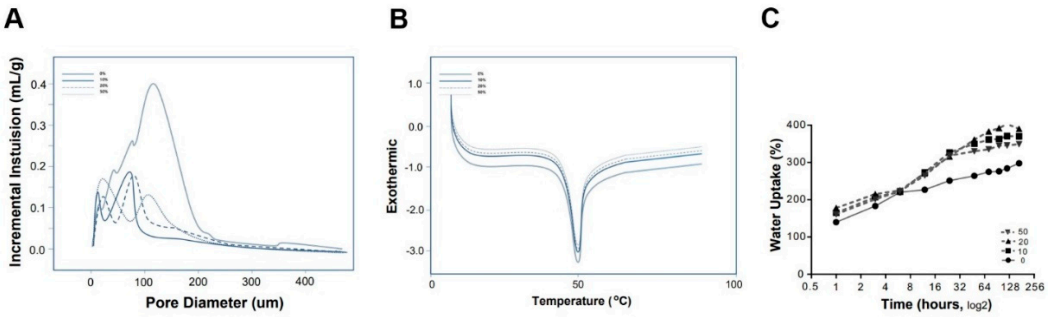

Figure 4. Properties of the CMC scaffold. (A) Mercury porosimetry analysis displays the pore size distributions of fibroin and fibroin/CMC scaffolds. 0 %, fibroin only; 10 %, fibroin/CMC (10 wt %); 20 %, fibroin/CMC (20 wt %); and 50 %, fibroin/CMC (50 wt %). (B) Differential scanning calorimetry were measured in each DSC thermogram of fibroin scaffold and scaffolds with various concentration of CMC. 0 %, fibroin only; 10 %, fibroin/CMC (10 wt %); 20 %, fibroin/CMC (20 wt %); and 50 %, fibroin/CMC (50 wt %). (C) Absorption rate was evaluated as water-uptake ability of the scaffold with respect to CMC concentration. 0 %, fibroin only; 10 %, fibroin/CMC (10 wt %); 20 %, fibroin/CMC (20 wt %); and 50 %, fibroin/CMC (50 wt %).

However, analysis of the porosity and median pore size showed no significant difference with respect to the content of fibroin. When the fibroin content was significantly increased, a small difference in pore size was observed. As the fibroin content is increased, the protein is expected to block the periphery of the pores slightly. However, the concentration is within a range that does not significantly affect the adhesion and growth of cells. A porosity of 65 % or more was observed in all samples, thereby confirming that a support with a constant size and porosity was prepared even after the addition of fibroin (Figure 4A), consistent with a previous report [34]. Differential scanning calorimetry was performed to observe the thermal behavior of the scaffold according to the CMC content. The melting point of each sample was above 50 °C, and the melting points of fibroin and CMC-containing scaffolds were almost the same (Figure 4B).

The hydrophilic effect observed that the scaffold containing CMC had a moisture content of approximately 430 %, and the fibroin scaffold without CMC had a maximum moisture content of 320 % (Figure 4C). The initial moisture content was high in 50 wt % fibroin/CMC scaffold. However, after 48 h, the moisture content was lower than that in the 10 or 20 wt % fibroin/CMC scaffold. Hence, 50 wt % fibroin scaffold contained two to four-fold higher fibroin content than other samples of the same volume and showed a lower absorption rate than 10 or 20 wt % fibroin/scaffold after a certain period due to its high density. The higher water content of the CMC scaffold can be attributed to hydrophilic amino acids, such as glutamic acid, arginine, and cysteine, which are major components of fibroin [35].

3.4. Identification of BMSCs under the Fibroin/CMC Scaffold

BMSCs were isolated from the femur and cultured for approximately three passages. Cellular morphology was analyzed after three weeks to assess mesenchymal stem cell development. Histological staining of MSC to differentiate into bone. The von Kossa-stained MSCs were visualized in black by silver nitrate. Von Kossa staining confirmed the presence of mesenchymal stem cells derived from rat bone marrow (Figure 5A).

Preprints (www.preprints.org) | NOT PEER-REVIEWED | Posted: 26 June 2023 doi:10.20944/preprints202306.1795.v1

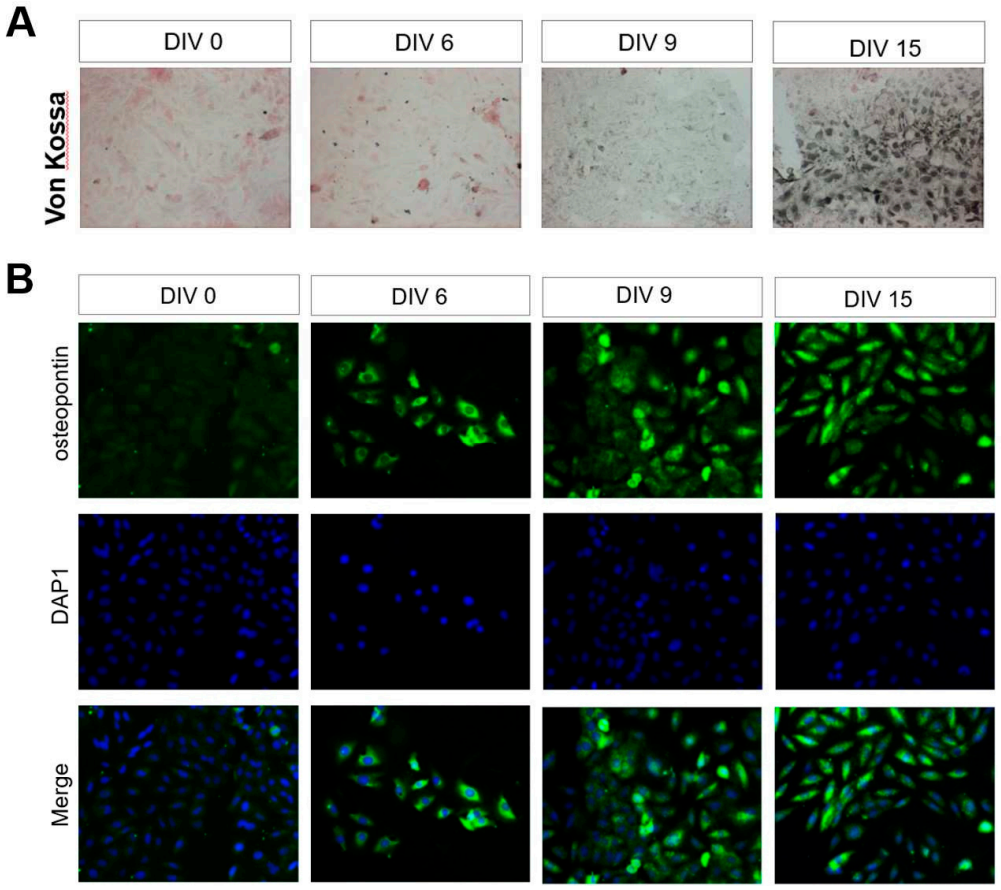

Figure 5. Identification of BMSCs. (A) Histological staining of MSC to differentiate into bone. The von Kossa stained cells (MSCs) were visualized in black by silver nitrate. (B) Further analysis of MSC was shown in Immunofluorescence staining of osteopentin. Immunofluorescence was visualized using FITC (green) and the nuclei by DAPI (blue). The morphology of which was primarily spindle-shaped and polygonal.

On the day of 12 after culture, the mesenchymal stem cells exhibited highly expression of each bone-related protein, osteopontin (Figure 5B). The osteogenic differentiation effect of the CMC scaffold on BMSCs was evaluated through osteopontin immunocytochemistry of oseopontin, showing changes over time (Figure 5B) Figure 2**.** This is a figure. Schemes follow another format. If there are multiple panels, they should be listed as: (**a**) Description of what is contained in the first panel; (**b**) Description of what is contained in the second panel. Figures should be placed in the main text near to the first time they are cited. A caption on a single line should be centered.

3.5. The Beneficial Effect of CMC Scaffold on Osteogenic Differentiation

The growth of BMSCs in scaffolds with various CMC contents was compared using MTT analysis. Cytotoxicity was not detected in CMC-containing scaffold or the fibroin scaffold alone (Figure 6A).

Preprints (www.preprints.org) | NOT PEER-REVIEWED | Posted: 26 June 2023 doi:10.20944/preprints202306.1795.v1

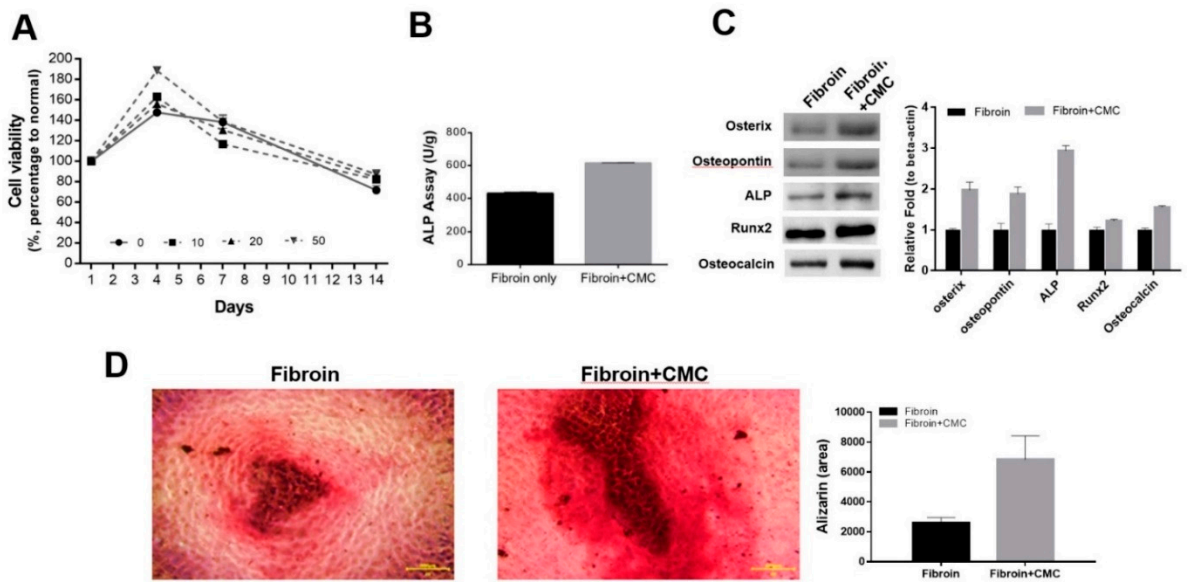

Figure 6. The beneficial effect of CMC scaffold on osteogenic differentiation. (A) The viability of bone marrow mesenchymal stem cells was measured by culturing the cells on fibroin and fibroin/CMC scaffolds. Cell viability did not differ between fibroin and fibroin/CMC scaffolds. CMC concentrations of 10 mg/ml and 20 mg/ml were considered suitable for cell survival. (B) ALP activity was measured in each fibroin only and CMC added fibroin scaffold. (C) Osteogenic differentiation of bone marrow mesenchymal stem cells was evaluated. In western blot analysis, bone-related protein expression amounts were evaluated by western blot analysis of bone marrow mesenchymal stem cells (left) and it is presented in the quantitative graph (right). (D) Bone nodule was stained with alizarin red S in two groups of fibroin only and fibroin with CMC (left). The formed nodules were quantified the by stained area and optical density (right).

Particularly, in 10 or 20 wt % fibroin/CMC scaffold, the viability of BMSCs showed a slight increase. ALP activity, an extracellular enzyme produced by osteoblasts and an indicator of bone formation, was assessed in BMSCs that seeded on the prepared fibroin/CMC scaffold. The activity of ALP, an early marker of osteo-differentiation, was starting to rise in scaffolds containing CMC on the first day (data not shown). The final ALP activity at day 14 was increased in higher in the scaffold containing CMC than that in the scaffold containing fibroin alone (Figure 6B). Since the scaffold containing CMC demonstrated differentiation into osteocytes, the ALP activity corresponding to differentiation into osteoblasts may increase, as previously reported [36]. Furthermore, to confirm the phenotype of BMSCs on fibroin/CMC scaffolds, proteins related to osteoblasts were analyzed by western blotting. The protein levels of osteocytic markers, such as osterix, osteopontin, ALP, Runx2, and osteonectin were showed a higher increase in the scaffold with a CMC concentration of 50 % than that in the scaffold with no CMC compared to the control group (Figure 6C). To confirm the effect of each scaffold on osteocyte differentiation, Alizarin Red was used. Calcium staining using the alizarin red S was performed at day 14 in each fibroin or CMC added fibroin sample to confirm forming bone nodule (Figure 6D, left). The bone nodule was semi-quantified by red stained area, and the area was shown in the graph (Figure 6D, right). After 14 days of culture, it was confirmed that Fibroin + CMC (50 %) differentiated into osteocytes more than fibroin alone, and differentiation started after 2 weeks.

4. Discussion

The physical properties of the CMC and fibroin polymer were mechanically, chemically, and biologically analyzed in this study. The CMC added scaffold facilitated effect on bone differentiation and play an important role in facilitating cartilage, ossification, and nerve differentiation of BMSCs.

The solvent-casting freeze drying method proved to be effective in fabricating a porous scaffold containing fibroin, as the scaffold maintained its external shape and exhibited no defects, highlighting its structural integrity (Figure 1). The SEM image of the prepared porous fibroin/CMC scaffold confirmed that the porous shapes of the inner and side were not different (Figure 2). The similarity between the porous shapes of the support and the salt particles suggests successful replication of the desired morphology. Additionally, no significant morphological difference indicates that the

presence of fibroin had minimal impact on the overall porous structure during the preparation process. These results demonstrate the successful fabrication of the porous scaffold and the suitability of fibroin as a component in its production and supports the suitability of fibroin as a component in the fabrication of the porous scaffold. (Figure 2).

In H-NMR spectrum data, the change in the substitution degree of the catechol group in fibroin/CMC was according to the amount of CMC in an aqueous solution of pH 5.5, and the degree of substitution increased as the increasing amount of CMC (Figure 3). At an input amount of 1 g or more, however, there was no significant change but the substitution degree of catechol group was changed by increasing the pH from 5.5 to 7.5. Since fibroin had low solubility in water at neutral pH, the degree of substitution was lower at pH 6.5 than that observed at pH 5.5. However, at pH 7.5, the degree of substitution was slightly reduced owing to low reaction with the amine group of fibroins, which was attributed to partially oxidized CMC. Therefore, the amount of CMC (1 g) and pH (6.5) were fixed as the reaction conditions for fibroin/CMC with a maximum degree of substitution of 38.6 % (Figure 3).

Differential scanning calorimetry showed that CMC did not significantly affect the properties of the fibroin scaffold and can remain thermally stable (Figure 4). In the fibroin scaffold, the dye did not penetrate the scaffold even after 20 min; however, it almost completely penetrated the scaffold containing CMC. In addition, as the CMC content increased, the penetration rate also increased, which is thought to be due to increased hydrophilicity, as CMC itself is composed of amino acids, which are known to form proteins.

Under the fibroin added with CMC, the expression of each bone-related protein in BMSCs was observed on the day 6 of culture, but it was hardly expressed on the day 3 (Figure 5). In MTT assay, the viability of BMSCs showed a slight increase (Figure 6). This is because for cells to attach to the material, serum protein must be adsorbed to the material. Owing to its hydrophobic surface, CMC imparted hydrophilicity to the fibroin scaffold, with no direct interaction between the cell and the material, thereby inducing serum protein adsorption. This effect was considered beneficial for cell viability. The positive effect on the growth and proliferation of these cells could be attributed to the biocompatibility and hydrophilicity of fibroin. This should be considered an important factor in the design of future fibroin/CMC scaffolds. Currently, we have been studying on the preparation of various carriers containing fibroin and the effects of fibroin on the cartilage, ossification, and nerve differentiation of BMSCs, and expect them to apply on stem cells differentiation.

5. Conclusions

This study focused on the facilitating effect of the CMC added scaffold on bone differentiation. Fibroin is a useful biomaterial and is a major component of silk yarns composed of fibrous proteins. Improving for binding efficiency in bone formation after implanted scaffold, CMC was added to fibroin. Fibroin scaffolds containing CMC components promoted differentiation of bone marrow stem cells into osteocytes and showed superior biocompatibility than fibroin alone scaffolds. Our results showed that the CMC scaffold could play an important role in facilitating cartilage, ossification, and nerve differentiation of BMSCs, which could supply a potential application of such scaffolds in regenerative medicine.

Author Contributions: Conceptualization, W.J.L. and G.W.K.; methodology, W.J.L.; validation, W.J.L. and K.C.; formal analysis, W.J.L.; investigation, A.Y.K.; data curation, K.C.; writing—original draft preparation, W.J.L. and K.C.; writing—review and editing, K.C.; supervision, G.W.K. and K.C. All authors have read and agreed to the published version of the manuscript.

Funding: This research received no external funding.

Conflicts of Interest: The authors declare no conflict of interest.

References

1. Ghostine, S., et al., Long-term efficacy of myoblast transplantation on regional structure and function after myocardial infarction. Circulation, 2002. 106(12 Suppl 1): p. I131-6.
2. Gojo, S., et al., Transplantation of genetically marked cardiac muscle cells. J Thorac Cardiovasc Surg, 1997. 113(1): p. 10-8.

3. Jain, M., et al., Cell therapy attenuates deleterious ventricular remodeling and improves cardiac performance after myocardial infarction. Circulation, 2001. 103(14): p. 1920-7.
4. Li, R.K., et al., Cardiomyocyte transplantation improves heart function. Ann Thorac Surg, 1996. 62(3): p. 654-60; discussion 660-1.
5. Muller-Ehmsen, J., et al., Survival and development of neonatal rat cardiomyocytes transplanted into adult myocardium. J Mol Cell Cardiol, 2002. 34(2): p. 107-16.
6. Orlic, D., et al., Bone marrow cells regenerate infarcted myocardium. Nature, 2001. 410(6829): p. 701-5.
7. Reinecke, H., et al., Survival, integration, and differentiation of cardiomyocyte grafts: a study in normal and injured rat hearts. Circulation, 1999. 100(2): p. 193-202.
8. Reinecke, H. and C.E. Murry, Transmural replacement of myocardium after skeletal myoblast grafting into the heart. Too much of a good thing? Cardiovasc Pathol, 2000. 9(6): p. 337-44.
9. Sakai, T., et al., Fetal cell transplantation: a comparison of three cell types. J Thorac Cardiovasc Surg, 1999. 118(4): p. 715-24.
10. Scorsin, M., et al., Does transplantation of cardiomyocytes improve function of infarcted myocardium? Circulation, 1997. 96(9 Suppl): p. II-188-93.
11. Liuyun, J., L. Yubao, and X. Chengdong, Preparation and biological properties of a novel composite scaffold of nano-hydroxyapatite/chitosan/carboxymethyl cellulose for bone tissue engineering. J Biomed Sci, 2009. 16(1): p. 65.
12. Zheng, S., et al., Gene-modified BMSCs encapsulated with carboxymethyl cellulose facilitate osteogenesis in vitro and in vivo. J Biomater Appl, 2021. 35(7): p. 814-822.
13. Zhang, M., et al., Cardiomyocyte grafting for cardiac repair: graft cell death and anti-death strategies. J Mol Cell Cardiol, 2001. 33(5): p. 907-21.
14. Reinecke, H. and C.E. Murry, Taking the death toll after cardiomyocyte grafting: a reminder of the importance of quantitative biology. J Mol Cell Cardiol, 2002. 34(3): p. 251-3.
15. Leor, J., et al., Bioengineered cardiac grafts: A new approach to repair the infarcted myocardium? Circulation, 2000. 102(19 Suppl 3): p. III56-61.
16. Kellar, R.S., et al., Scaffold-based three-dimensional human fibroblast culture provides a structural matrix that supports angiogenesis in infarcted heart tissue. Circulation, 2001. 104(17): p. 2063-8.
17. Thompson, W.D., et al., Angiogenic activity of fibrin degradation products is located in fibrin fragment E. J Pathol, 1992. 168(1): p. 47-53.
18. Bootle-Wilbraham, C.A., et al., Fibrin fragment E stimulates the proliferation, migration and differentiation of human microvascular endothelial cells in vitro. Angiogenesis, 2001. 4(4): p. 269-75.
19. Naito, M., et al., Smooth muscle cell outgrowth stimulated by fibrin degradation products. The potential role of fibrin fragment E in restenosis and atherogenesis. Thromb Res, 2000. 98(2): p. 165-74.
20. Dvorak, H.F., et al., Fibrin containing gels induce angiogenesis. Implications for tumor stroma generation and wound healing. Lab Invest, 1987. 57(6): p. 673-86.
21. Christman, K.L., et al., Fibrin glue alone and skeletal myoblasts in a fibrin scaffold preserve cardiac function after myocardial infarction. Tissue Eng, 2004. 10(3-4): p. 403-9.
22. Sievers, R.E., et al., A model of acute regional myocardial ischemia and reperfusion in the rat. Magn Reson Med, 1989. 10(2): p. 172-81.
23. Wolfe, C.L., et al., Assessment of myocardial salvage after ischemia and reperfusion using magnetic resonance imaging and spectroscopy. Circulation, 1989. 80(4): p. 969-82.
24. Zhu, B., et al., Comparative effects of pretreatment with captopril and losartan on cardiovascular protection in a rat model of ischemia-reperfusion. J Am Coll Cardiol, 2000. 35(3): p. 787-95.
25. Zhu, B., et al., Effects of different durations of pretreatment with losartan on myocardial infarct size, endothelial function, and vascular endothelial growth factor. J Renin Angiotensin Aldosterone Syst, 2001. 2(2): p. 129-33.
26. Rando, T.A. and H.M. Blau, Primary mouse myoblast purification, characterization, and transplantation for cell-mediated gene therapy. J Cell Biol, 1994. 125(6): p. 1275-87.
27. Fishbein, M.C., D. Maclean, and P.R. Maroko, Experimental myocardial infarction in the rat: qualitative and quantitative changes during pathologic evolution. Am J Pathol, 1978. 90(1): p. 57-70.
28. Zahedi, M., et al., Equine bone marrow-derived mesenchymal stem cells: optimization of cell density in primary culture. Stem Cell Investig, 2018. 5: p. 31.
29. Kloner, R.A., et al., Intramyocardial injection of DNA encoding vascular endothelial growth factor in a myocardial infarction model. J Thromb Thrombolysis, 2000. 10(3): p. 285-9.
30. Li, W., et al., Role of MMPs and plasminogen activators in angiogenesis after transmyocardial laser revascularization in dogs. Am J Physiol Heart Circ Physiol, 2003. 284(1): p. H23-30.
31. Havenith, M.G., et al., Muscle fiber typing in routinely processed skeletal muscle with monoclonal antibodies. Histochemistry, 1990. 93(5): p. 497-9.

 doi:10.20944/preprints202306.1795.v1

32. Benjamin, L.E., I. Hemo, and E. Keshet, A plasticity window for blood vessel remodelling is defined by pericyte coverage of the preformed endothelial network and is regulated by PDGF-B and VEGF. Development, 1998. 125(9): p. 1591-8.
33. Zhou, L., et al., X-ray photoelectron spectroscopic and Raman analysis of silk fibroin-Cu(II) films. Biopolymers, 2006. 82(2): p. 144-51.
34. Thiagarajan, P., A.J. Rippon, and D.H. Farrell, Alternative adhesion sites in human fibrinogen for vascular endothelial cells. Biochemistry, 1996. 35(13): p. 4169-75.
35. Vailhe, B., et al., In vitro angiogenesis is modulated by the mechanical properties of fibrin gels and is related to alpha(v)beta3 integrin localization. In Vitro Cell Dev Biol Anim, 1997. 33(10): p. 763-73.
36. Sahni, A., T. Odrljin, and C.W. Francis, Binding of basic fibroblast growth factor to fibrinogen and fibrin. J Biol Chem, 1998. 273(13): p. 7554-9.